Journal of Solution Chemistry (2021) 50:315–339
https://doi.org/10.1007/s10953-021-01055-w

Acid Dissociation Constants, Enthalpy, Entropy and Gibbs Energy of Bedaquiline by UV-Metric Spectral and pH-Metric Analysis

Milan Meloun[1] · Daniela Cyrmonová[1] · Milan Javůrek[2] · Tomáš Pekárek[3]

Received: 28 May 2020 / Accepted: 7 October 2020 / Published online: 5 March 2021

Abstract
Bedaquiline (trade name Sirturo) is an antibiotic used to treat pulmonary tuberculosis that is resistant to other antibiotics. The pH-spectrophotometric and pH-potentiometric titrations allowed the measurement of two near successive and one distant dissociation constants. The neutral bedaquiline LH molecule was able to protonate and dissociate in pure water to form soluble species L^-, LH, LH_2^+, LH_3^{2+} and LH_4^{3+}. In the pH range 2–7, three dissociation constants can be reliably estimated. REACTLAB (UV-metric spectral analysis) values are: $pK_{a1}^T = 3.91(09)$, $pK_{a2}^T = 4.58(12)$ and $pK_{a3}^T = 5.26(07)$ at 25 °C and $pK_{a1}^T = 3.61(30)$, $pK_{a2}^T = 4.44(15)$ and $pK_{a3}^T = 5.54(33)$ at 37 °C. ESAB (pH-metric analysis) values are: $pK_{a1}^T = 3.21(39)$, $pK_{a2}^T = 3.68(31)$ and $pK_{a3}^T = 5.21(42)$ at 25 °C and $pK_{a1}^T = 3.31(12)$, $pK_{a2}^T = 3.67(15)$ and $pK_{a3}^T = 5.73(08)$ at 37 °C. Molar enthalpy ΔH^0, molar entropy ΔS^0 and Gibbs energy ΔG^0 were calculated from the spectra using the dependence of ln K on $1/T$. The potentiometric data showed positive enthalpy $\Delta H^0(pK_{a1}) = 85.49$ kJ·mol^{-1}, $\Delta H^0(pK_{a2}) = 86.42$ kJ·mol^{-1}, and $\Delta H^0(pK_{a3}) = 65.84$ kJ·mol^{-1} values and the dissociation reactions were endothermic. The entropy ΔS^0 at 25 °C was positive for the three dissociation constants $\Delta S^0(pK_{a1}) = 217.47$ J·K^{-1}·mol^{-1}, $\Delta S^0(pK_{a2}) = 204.87$ J·K^{-1}·mol^{-1}, and $\Delta S^0(pK_{a3}) = 92.63$ J·K^{-1}·mol^{-1} at 25 °C and proved irreversible dissociation reactions.

✉ Milan Meloun
milan.meloun@upce.cz
http://meloun.upce.cz
http://www.upce.cz

Daniela Cyrmonová
daniela.cyrmonova@upce.cz

Milan Javůrek
milan.javurek@upce.cz
http://www.upce.cz

Tomáš Pekárek
tomas.pekarek@zentiva.com
http://www.zentiva.com

[1] Department of Analytical Chemistry, University of Pardubice, 532 10 Pardubice, Czech Republic

[2] Department of Process Control, University of Pardubice, 532 10 Pardubice, Czech Republic

[3] Zentiva, k. s., U Kabelovny 130, 102 37 Prague, Czech Republic

Graphic Abstract

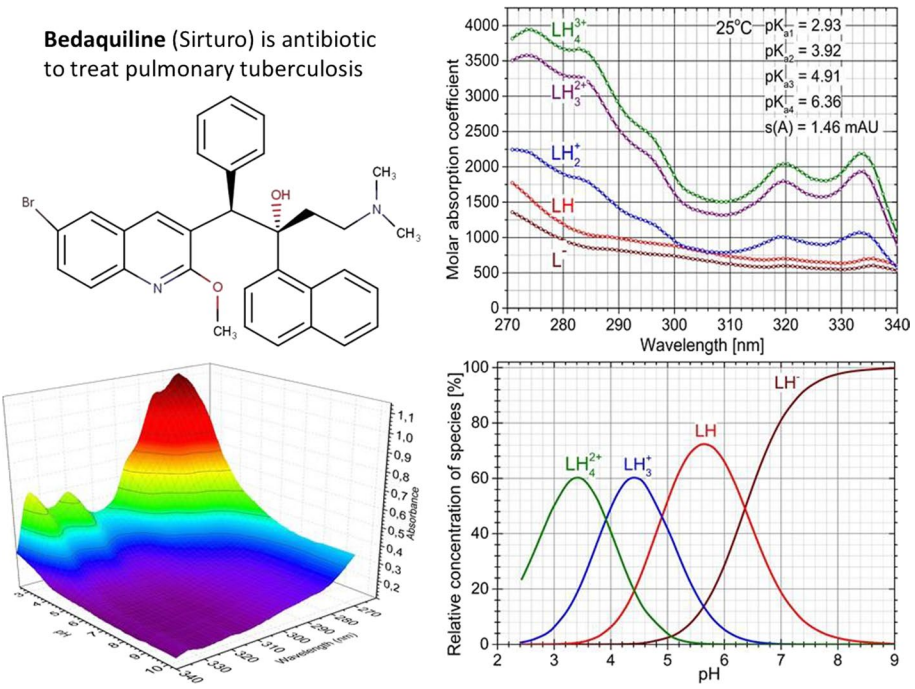

Keywords Dissociation constants · Bedaquiline · Spectrophotometric titration · pH-titration · REACTLAB · SQUAD84 · ESAB

1 Introduction

Bedaquiline, chemically (1*R*,2*S*)-1-(6-bromo-2-methoxyquinolinyl-3-yl)-4-(dimethylamino)-2-naphthalenyl)-1-yl-1-phenylbutan-2-ol, of the trade name *Sirturo*, is an antibiotic used, along with other drugs, to treat pulmonary tuberculosis that is resistant to other antibiotics. Bedaquiline is of the chemical formula $C_{32}H_{31}BrN_2O_2$ with a molecular weight of 555.5 g·mol^{-1}; its structure is shown in Fig. 1. It was registered under DrugBank ID 08903 on November 2016 under the CAS number 843663-66-1 and its PubChem CID is 5388906. It possesses the UNII 78846I289Y [1]. The drug was approved on December 2012 by the American Food and Drug Administration (FDA) for the treatment of multidrug-resistant tuberculosis as part of a Fast-Track accelerated approval, for use only in cases of multidrug-resistant tuberculosis. Multidrug-resistant tuberculosis is a type that is resistant to isoniazid and rifampicin, which are the two most effective first-line antituberculars.

Bedaquiline is the first member of a new class of drugs called diarylquinolines which block the proton pump of *Mycobacterium tuberculosis* ATP synthase. There are two mechanisms for blocking the bedaquiline pump in *M. tuberculosis* [1, 2]. The first mechanism is the direct binding of bedaquiline to the c subunit of ATP bacterial synthesis. This

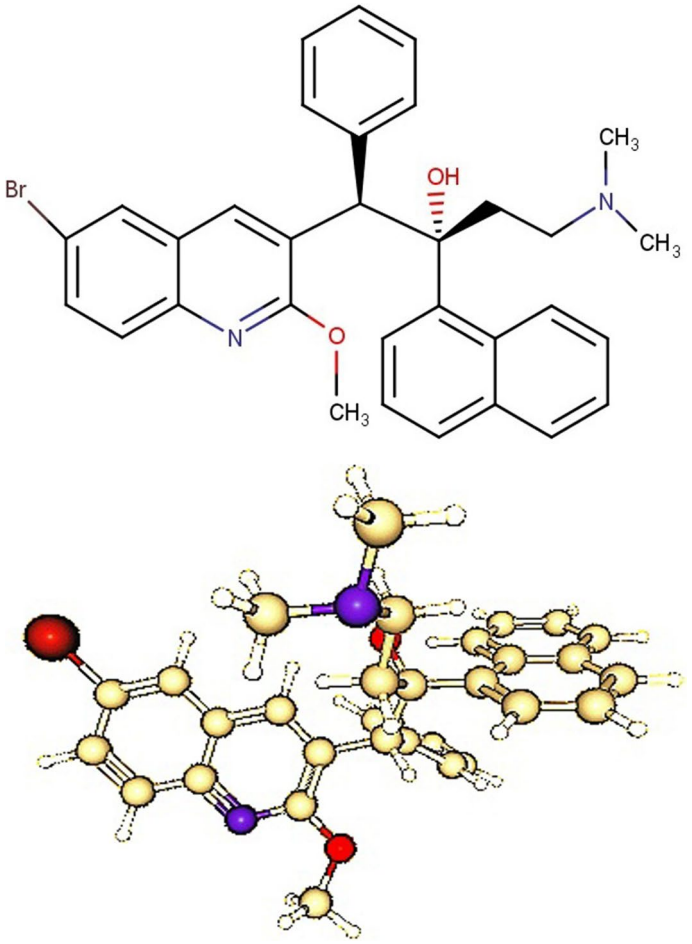

Fig. 1 Structural formula of bedaquiline

inactivates this enzyme, which catalyzes the synthesis of ATP. The second, indirect mechanism, involves bedaquiline-induced electron transport in the electron transport chain on ATP synthase. The production of ATP is essential for cell life, and its loss leads to inhibition of mycobacterial growth within a few hours after bedaquiline administration [2–4].

Bedaquiline is primarily exposed to oxidative metabolism, leading to the formation of the *N*-monodesmethyl metabolite (M2) which is considered not to contribute significantly to clinical efficacy due to its lower average human exposure and lower antimycobacterial activity (4–6 times lower) compared to the parent compound [1, 3, 5].

Following a single oral dose of Sirturo, peak plasma concentrations of c_{max} are usually reached approximately 5 h after dosing. The maximum plasma concentration of bedaquiline is 1.659 ng·mL^{-1}. Administration of the drug with a standard meal containing approximately 22 g of fat increased the relative bioavailability by approximately twofold compared to administration in a fasted state. The plasma protein binding of bedaquiline is greater than 99.9%. Thus, bedaquiline is transported by the blood by binding to proteins. After reaching the c_{max}, the bedaquiline concentration exponentially decreases three times. The

mean terminal elimination half-life of bedaquiline and the *N*-monodesmethyl metabolite (M2) is approximately 5.5 months. This long terminal elimination phase probably reflects the slow release of bedaquiline and M2 from peripheral tissues. However, plasma M2 concentrations appear to correlate with QT prolongation. Bedaquiline is metabolized in the liver. The major enzyme involved is CYP3A4, which metabolises bedaquiline to the *N*-monodesmethyl metabolite (M2). This metabolite is 4–6 times less active in terms of antimycobacterial activity [5].

Like any medicine, bedaquiline has a number of side effects. Common side effects include nausea, joint pain, headache and chest pain. Other side effects may include liver failure, elevated liver enzymes such as elevated serum alanine aminotransferase, elevated serum aspartate aminotransferase, elevated serum transaminase, and anorexia [6].

One of the most important physicochemical properties of each drug is the values of its dissociation constants. Protonation equilibria and ionization of the drug are particularly important for predicting its behavior under physiological conditions, as the ionization state strongly affects the solubility at the site of application [7, 8].

1. The acid dissociation constants of the acid LH_j can be determined by regression analysis of potentiometric titration data, also called pH-metric analysis [9–15], in which the common parameters (pK_{ai}, $i = 1, \ldots, j$) and the group parameters (E^0, L_0, H_T) are simultaneously numerically refined. Comparisons are often made of estimates of unknown parameters, quantified by regression programs of pH-potentiometric titration data, applications of ESAB [12], SUPERQUAD and HYPERQUAD [13–15].
2. The pH-spectrophotometric analysis, also called the UV-metric spectral analysis [16, 17] is a particularly highly sensitive and frequently used method for determining pK_a in very dilute aqueous solutions, as it requires simpler equipment and can operate with sub-micromolar concentrations (about 10^{-5} mol·dm^{-3} to 10^{-6} mol·dm^{-3}).
3. The accuracy of theoretical quantum-chemical predictions of estimates of pK_a in a protonation model from the structural formula of a drug molecule is based on three predictive programs: PALLAS [18, 19], ACD/Percepta [20–23] and MARVIN [24–26], which are often confirmed as the best of the nine available prediction programs [27].

The aim of this study was to conduct a regression analysis of the pH-absorbance matrix with very small changes in absorbance in the pH-spectra of bedaquiline and also to evaluate an alternative pH-metric potentiometric titration curve of the protonation model in order to optimize experimental conditions for determining several closely successive dissociation constants and enthalpy, entropy and Gibbs energy. Detailed instructions for titrating the UV/VIS pH-absorption spectra, called UV-metric spectral analysis and alternatively pH-metric analysis, were previously described in a 10-step procedure [26, 28–30].

2 Computer Data Analysis

To construct a regression protonation model for pH-spectrophotometric titration data, it is often necessary to make a number of adjustments to the appropriate numerical analysis strategy of the instrumental data to avoid negative estimates of some parameters, such as molar absorption coefficients. The procedure of pH-titration of UV/VIS-absorbance spectra called the UV-metric spectral analysis [16], and the alternatively used pH-metric titration analysis [29], have been previously described in a 10-step tutorial [29–31]. Both

instrumental methods can be used not only to determine the dissociation constants but also to quantify the standard state enthalpy ΔH^0, entropy ΔS^0 and Gibbs energy ΔG^0, even for sparingly soluble drugs. To properly understand their acidic behavior, it is very important to investigate the entropic and enthalpy properties of the dissociation process of the drugs in water [32].

The concept of QSAR/QSPR [33] is used to transform the search for compounds with the desired properties by chemical intuition quantified into mathematical form. Protonation energy can be considered as a good measure of the strength of hydrogen bonds, since the higher the energy, the stronger the bond [34–37]. The relationships between these estimated thermodynamic parameters are called "extra-thermodynamics" for many reactions. Enthalpy–entropy compensation is a widely observed effect in physical, biological, chemical and biochemical processes [38–40] and is well described by Liu and Guo [41]. If there is a change in certain conditions such as pH, solvent composition, reactant molecule, water activity, ionic hydration or hydrogen bond, the enthalpy and entropy of activation will change accordingly.

The quantitative relationship between the structure and QSAR activity [33] elucidates the importance of different structural interactions between a drug molecule and a proton. The Gibbs energy ΔG^0 can be divided into two terms, $\Delta G^0 = \Delta H^0 - T\Delta S^0$, i.e., the enthalpy ΔH^0 and the entropic term ΔS^0.

The change in enthalpy ΔH^0 represents the amount of energy that is added $\Delta H^0 > 0$ (endothermic reaction) or released $\Delta H^0 < 0$ (exothermic reaction). In pharmacological studies, ΔH^0 is commonly interpreted as a reflection of changes in intermolecular forces between drug and proton or hydrogen bonds with van der Waals interactions. The van't Hoff's equation,

$$\frac{d \ln K_{ai}}{dT} = \frac{\Delta H^0}{RT^2}$$

where $R = 8.31451\ \mathrm{J{\cdot}K^{-1}{\cdot}mol^{-1}}$ is an ideal gas constant, is often integrated in practice between two temperatures, assuming that the enthalpy of the reaction ΔH^0 (here it is a protonation) is constant. The data should show a linear relationship

$$\ln K = -\frac{\Delta H^0}{RT} + \frac{\Delta S^0}{R}$$

where the term $-\Delta H^0/R$ is the slope and the term $\Delta S^0/R$ is the intercept of the linear relationship. Evaluating the slope and the intercept from the van't Hoff equation will allow the quantification of the enthalpy and entropy of the protonation.

The change in entropy ΔS^0 can be seen as a measure of the unpredictability of molecular positions, uncertainty, "disturbances," "randomness," or statistically, as the number of possible microscopic states or molecular configurations of a reversible reaction. In pharmacological studies, entropy is often interpreted as a measure of rearrangement in solvent (water) molecules. Entropy can be expressed by the relation $\Delta S^0 = 1/T\,(\Delta H^0 + RT \ln K)$.

The change in Gibbs energy ΔG^0 represents the amount of work, but work other than the work of expansion. By modifying the Gibbs energy definition of $\Delta G^0 = \Delta H^0 - T\Delta S^0$, where ΔS^0 is the entropy of the system, the Gibbs energy isotherm will then be expressed by the relation $\Delta G^0 = -RT \ln K$. Chemical reactions (here dissociation) are called *exergonic* when $\Delta G^0 < 0$ and *endergonic* when $\Delta G^0 > 0$.

Extrathermodynamics of dissociation: The linear relationship between the enthalpy change member ΔH^0 [$\mathrm{kJ{\cdot}mol^{-1}}$] and the entropy change member ΔS^0 [$\mathrm{kJ{\cdot}K^{-1}{\cdot}mol^{-1}}$]

means that enthalpy changes are compensated by changes in entropy (or vice versa) so that the change in Gibbs energy ΔG^0 [kJ·mol^{-1}] remain constant. In practice, the obtained linear relationship can take the form $\alpha = \Delta H° - \beta \Delta S°$, where β is not necessarily equal to T. For this compensatory effect, the correlation coefficient of linear dependence is used as a criterion and the higher the correlation coefficient, the better is the compensation.

3 Materials and Methods

3.1 Materials

Bedaquiline, sponsored by ZENTIVA, k. s. (Prague), has a declared purity controlled by the HPLC method and alkalimetry, of always > 99%. This drug was always weighed directly in a reaction vessel, resulting in a final analytical concentration of about 1.0×10^{-4} mol·dm^{-3}. Hydrochloric acid, 1 mol·dm^{-3}, was prepared by diluting concentrated HCl (p.a., Lachema Brno) with redistilled water and standardizing against HgO and KI with a repeatability that was expressed as "about exactly" better than 0.002 mol·dm^{-3} according to the equation $HgO + 4KI + H_2O \rightleftharpoons 2\ KOH + K_2[HgI_4]$ and $KOH + HCl \rightleftharpoons Cl + H_2O$. From the exact weight of the pellets, potassium hydroxide, 1 mol·dm^{-3}, is prepared, (p.a. Aldrich Chemical Company) with redistilled water without carbon dioxide, which had been kept for 50 min before in an ultrasonic bath. The solution was stored for several days in a polyethylene bottle under an argon atmosphere. It was standardized potentiometrically against a potassium hydrogen phthalate solution, and the equivalence point was evaluated using a derivative method with a reproducibility of 0.001 mol·dm^{-3}. Mercury oxide, potassium iodide and potassium chloride, (p. a., Lachema Brno) were not subjected to extra purification. Double redistilled water was kept for 50 min in a sonographic bath prior to the preparation of solutions.

3.2 Apparatus

The instrumentation used and both titration procedures were previously described in detail [20, 26, 29, 42, 43]. The concentration of hydrogen ions [H^+] was measured on a Hanna HI 3220 digital voltmeter with an accuracy of ± 0.002 pH using a combined glass electrode Theta HC 103-VFR. Potentiometric titrations of the acidified drug with hydrochloric acid to pH 2 were performed using the pa_{H+} hydrogen activity scale. pH meter standardization was performed using WTW buffer values, 4.006 (4.024), 6.865 (6.841) and 9.180 (9.088) at 25 °C and 37 °C (in parentheses).

pH-spectrophotometric titration with registration of the absorbance spectrum at 300 wavelengths was performed as follows: an aqueous solution of 20.00 cm^3 containing 10^{-4} mol·dm^{-3} of drug, 0.100 mol·dm^{-3} of hydrochloric acid, 2.44 μmol·dm^{-3} phosphate buffer and 10 cm^3 of indifferent KCl solution for ionic strength adjustment was titrated with the standard 1.0 mol·dm^{-3} KOH at 25 °C and 37 °C, and 80 absorption spectra were recorded. Titrations were performed in a glass vessel with a double-walled jacket filled with 100 cm^3 thermostated water, and the vessel was closed with a Teflon liner containing electrodes, an argon inlet, a thermometer, a propeller stirrer, and a hairy capillary mouth of a piston microburette. All pH measurements were performed at (25.0 ± 0.1) °C and (37.0 ± 0.1) °C. During drug titration, the solution was bubbled with a stream of argon to mix thoroughly and maintain an inert atmosphere. The argon was passed through an

aqueous ionic medium prior to passing through one or two wash vessels, which also contained a titration medium before entering the corresponding titrated solution. The microburettes used of a total volume of 1250 µL (META, Brno) were equipped with a micrometer screw of 25.00 cm [44]. The hair polyethylene capillary tip of the plunger microburette was immersed in the titrand solution during the titrant addition from microburette, but after each titrant addition, the tip was withdrawn from the titrand to prevent spontaneous leakage of the titrant during the pH read-out. The microburette was calibrated by determining the total volume of water supplied tenfold by weighing it on a Sartorius 1712 MP8 balance and the results evaluated statistically, resulting in an accuracy of ± 0.015% of the added volume over the entire titration range. After the pH adjustment in the reaction vessel, the solution was transported to the cuvette by a peristaltic pump, which was a part of the CINTRA 40 spectrophotometer (GBC, Australia), and the spectrum at 300 wavelengths was recorded.

3.3 Software

Numerical estimation of dissociation constants was performed by the nonlinear regression analysis of a set of 80 pH-absorbance spectra measured by UV-spectroscopy using two proven programs SQUAD84 [31, 45] and REACTLAB [46] and the potentiometric pH-titration curve using the program ESAB [12]. Spectral interpretation of the rank of the pH-absorbance matrix using the INDICES program [47] reliably determined the number of light-absorbing species n_c of the equilibrium mixture. Drug spectra plots were drawn by the program ORIGIN 9.1 [48]. The PALLAS [18, 19], ACD/Percepta [20–23] and MARVIN [24–26] programs were used to predict the dissociation constants and were based on the structural formula of bedaquiline.

4 Results and Discussion

Methods of numerical analysis of pH spectra and pH-potentiometric titration curves have proven to be the best instrumental methods since they also reliably determine close dissociation constants, even in the case of the poorly soluble drug bedaquiline. pH-spectrophotometric titration (called the UV-metric analysis) was used as an alternative method to pH-potentiometric titration (called the pH-metric analysis) to determine dissociation constants in the case of significantly high values of molar absorption coefficients and showed its high sensitivity to the substance concentration of bedaquiline around 10^{-4} mol·dm^{-3} of the otherwise poorly soluble drug.

4.1 UV-Metric Spectral Analysis

The experimental procedure and computational regression analysis strategy for determining dissociation constants by the UV-metric spectral analysis were described in 10 steps in the published tutorial [29] and is also available on page 226 in the textbook [31]. Generally, protonation model building and testing concerns the following calculations: determining the number of protonation equilibria, determining the number of differently protonated species, including their relative concentration diagram as well as the construction of a graph of their molar absorption coefficients versus measured wavelengths; the search model included statistical reliability criteria of the found regression model, including a number of statistical tests [49, 50].

4.1.1 Theoretical Prediction of the Dissociation Constants of Bedaquiline

The first step in the data analysis was the prediction of dissociation constants based on a quantum-chemical calculation and dealing with the structural formula of the studied drug molecule. The MARVIN prediction program identified three protonizable centers for bedaquiline that could theoretically be associated with up to three predicted dissociation constants (Fig. 2). This figure shows the interpretation of three dissociation constants in the distribution diagram. As both prediction programs, MARVIN and PALLAS, predicted dissociation constants that were slightly differing from each other, it was obvious that the experimental determination was necessary as it could offer more reliable estimates.

4.1.2 Determining the Number of Light-Absorbing Species n_c

Prior to the regression analysis of the pH-absorbance matrix, factor analysis should be applied to determine the rank of the second moment of the absorbance matrix to filter the significant eigenvalues (SVD) of the initial data. This factor analysis application was based on the fact that if the spectral data matrix consisted of r contributions from light-absorbing chemical species, then the first r factors of the absorbance matrix contained the vast majority of the chemical information obtained by the experiment. The value of r then denoted the rank of the matrix and should generally be less than or equal to the number of chemical

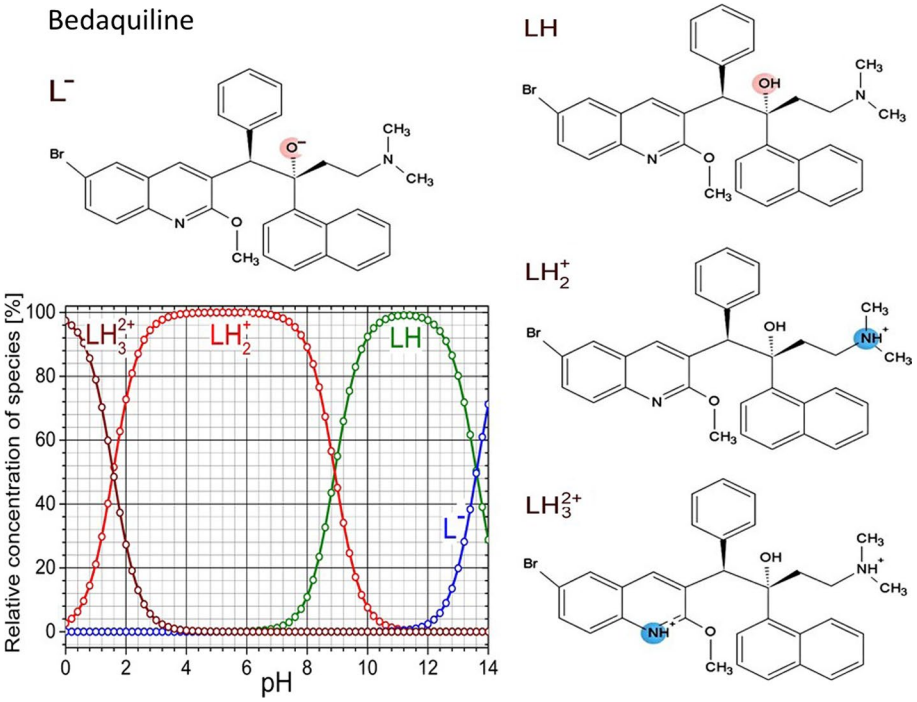

Fig. 2 Theoretical prediction of the dissociation constants of bedaquiline based on a structural formula with highlighted protonation centers and a distribution diagram of the relative concentrations (%) of variously protonated species L^-, LH, LiH_2^+, LH_3^{2+} for predicted dissociation constants using programs MARVIN and PALLAS

species *m*. Examination of the eigenvalues of the data matrix showed that the first several factors are of great importance until the break in the Cattel graph, from which the remaining factors were of negligible importance. These small values behind the break can in principle only represent the noise of the spectrophotometer, which numerically loaded the values of the spectrum. Removing these higher statistically insignificant factors from the spectral data created a factor model much closer to the chemical model with a number of chemical information.

Cattel's index graph of singular values (Fig. 3) showed that a set of bedaquiline spectra at wavelengths of 240–305 nm indicated four light-absorbing species in a mixture of $n_c = k^* = 4$ with an experimental noise level of $s_{inst}(A) = 1.14$ mAU; although the molar absorption coefficients of the first pair of LH^- and LH_2 species were unfortunately very similar. The true number of light-absorbing species separated from the spectral noise could then be reliably evaluated by non-linear regression analysis of spectral data in the building of a protonation model with the REACTLAB program.

4.1.3 Building and Testing the Protonation Model

In the REACTLAB program, a matrix of pH-absorbance spectra was evaluated by non-linear regression analysis, using a regression triplet method (data critique, model critique and method critique), cf. refs. [31, 49, 50]. The search for the best hypothesis of a protonation model containing two, three and four dissociation constants was shown in graphs of molar absorption coefficients (Fig. 4-*left*) and distribution diagrams of all protonated species (Fig. 4-*right*) for the tested protonation model. The reliability criterion of the best regression model sought was the goodness-of-fit test of the calculated spectra through the experimental spectra points, expressed by the standard deviation of the absorbance $s(A)$ in mAU from REACTLAB and from SQUAD in brackets.

Construction of a protonation model based on the goodness-of-fit test was a decisive criterion for accepting estimated unknown parameters, i.e. dissociation constants and molar absorption coefficients independence on wavelength with its statistical diagnostics for the tested hypothesis of a protonation model. It turned out that the construction of the protonation model of bedaquiline was not an easy task, because this molecule had two close successive dissociation constants ($|pK_{a2} - pK_{a1}| < 3$) and because the titration pH-change had only small effects on the absorbance changes of chromophores in the spectra. Therefore, both dissociation constants were poorly conditioned in the regression model and their determination was rather insensitive and therefore uncertain.

The criterion for searching the best hypothesis of the protonation model in construction of the regression model was the goodness-of-fit test of the calculated spectra through the experimental pH-absorbance matrix points, which could often be numerically simplified to examine the absorbance standard deviation value $s(A)$ after the minimization process termination in nonlinear regression, $s(A) = \sqrt{U_{min}(n-m)}$, where n was the number of experimental points and m was the number of estimated parameters [49].

Table 1 shows the numerical estimates of the dissociation constants calculated by the REACTLAB regression program, as well as the values of the arithmetic mean of all residuals $E(\hat{e})$ in mAU, the standard deviation of residuals $s(e)$ in mAU and the average of absolute values of residuals $E(|\hat{e}|)$. These statistics showed an excellent fit of the calculated spectra through the experimental absorbance points, which was achieved for

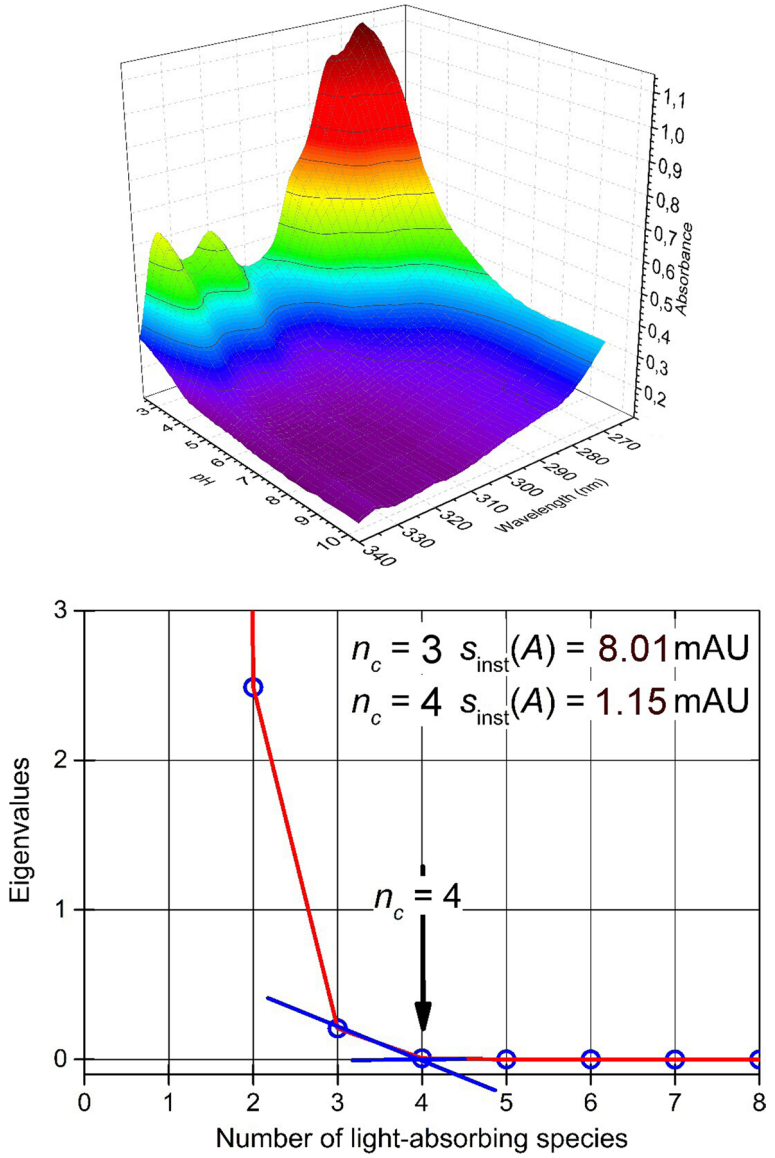

Fig. 3 *Upper graph* the 3D-absorbance response surface of bedaquiline as dependent on pH. *Lower graph* Cattel's eigenvalue index graph contains a break of the curve of the dependence of the eigenvalues of the pH-absorbance matrix on factors corresponding to the rank of the matrix $k^*=3$ or 4 and the number of light-absorbing species $n_c=3$ or 4 in comparison with the instrumental absorbance standard deviation $s_{inst}(A)$ (INDICES in S-PLUS)

the protonation model with three dissociation constants. The reliability of the calculated regression parameter estimates could be advantageously tested by assessing the regression diagnostics just presented (Table 1 and Fig. 4), as explained on page 226 in ref. [31]:

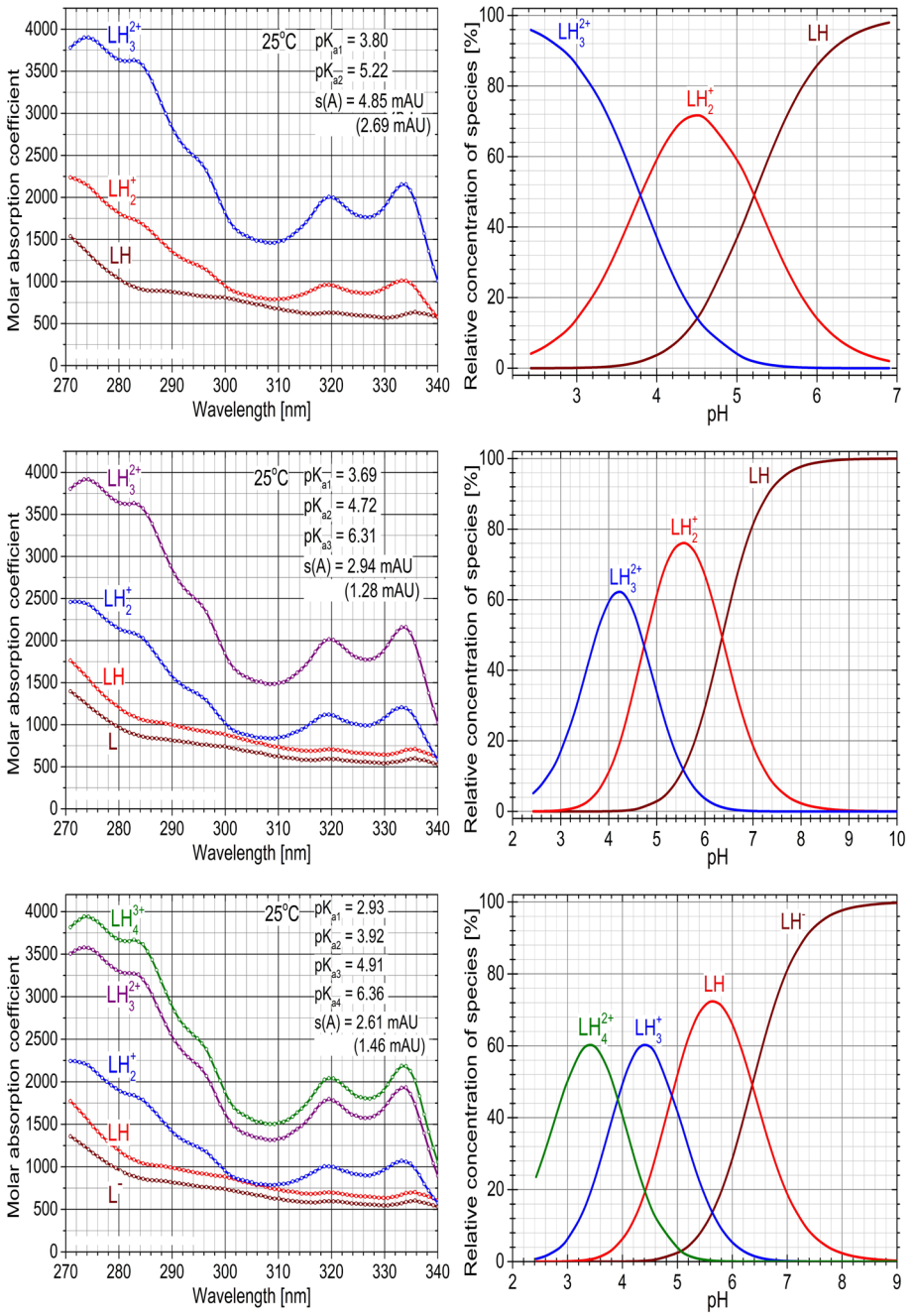

Fig. 4 Building and testing the best hypothesis of the proposed bedaquiline protonation model in the pH range of 2–10 indicated three or four dissociation constants pK_{a1}, pK_{a2}, pK_{a3} and pK_{a4}, by spectral analysis 1.0×10^{-4} mol·dm^{-3} bedaquiline at 25 °C. *Left graphs* pure spectral profiles of the molar absorption coefficients of differently protonated species ε_L, ε_{LH}, ε_{LH2}, ε_{LH3} and ε_{LH4} versus wavelength λ (nm), *Right graphs* the distribution diagrams of the relative concentrations of all variously protonated species as dependent on pH (REACTLAB, ORIGIN 9)

Table 1 Reproducibility of the best protonation model of bedaquiline in the pH range of 2–13 for the three dissociation constants pK_{a1}, pK_{a2}, pK_{a3} using REACTLAB at 25 °C and 37 °C

Temperature [C]	25 °C					37 °C				
Reproducibility	1st set	2nd set	3rd set	4rd set	Mean	1st set	2nd set	3rd set	4rd set	Mean
Cattel's scree plot indicating the rank of the absorbance matrix (INDICES)										
Number of spectra, n_s	34	22	38	44		34	35	34	31	
Number of wavelengths, n_w	146	130	164	106		128	117	128	117	
Number of light-absorbing species, k*	3	3	3	3		3	3	3	3	
Estimates of dissociation constants in the searched protonation model										
pK_{a1}, $LH_3^{2+} \rightleftharpoons H^+ + LH_2^+$	3.90	3.81	3.90	4.03	3.91	3.45	3.90	3.45	3.27	3.51
pK_{a2}, $LH_2^+ \rightleftharpoons H^+ + LH$	4.42	4.66	4.75	4.52	4.58	4.29	4.50	4.29	4.47	4.38
pK_{a3}, $LH \rightleftharpoons H^+ + L^-$	6.04	5.22	5.36	5.25	5.46	5.45	5.63	5.45	5.13	5.42
Goodness-of-fit test with the statistical analysis of residuals										
Residual standard deviation, $s(\hat{e})$, [mAU]	2.47	1.04	1.45	1.04		1.73	1.72	1.71	1.74	
Sigma from ReactLab, [mAU]	3.17	3.87	3.45	2.61		2.24	2.16	2.15	2.09	

Solutions of 1.0×10^{-4} mol·dm^{-3} bedaquiline at $I = 0.002$ mol·dm^{-3} were used for n_s spectra, measured at n_w wavelengths form differently protonated species. The resolution criterion and reliability of the parameter estimates obtained are proven with the goodness-of-fit statistics of the residuals analysis such as the standard deviation of the absorbance after the regression process $s(\hat{e})$ [mAU] and sigma $s(A)$ [mAU] from REACTLAB

(a) *Physical significance of estimates of unknown parameters* In the left part of Fig. 4 the spectra of molar absorption coefficients of variously protonated bedaquiline species are shown depending on the wavelength. If the pair of curves of molar absorption coefficients $\varepsilon = f(\lambda)$ is close or almost the same, the hypothesis of the determined protonation model may be uncertain or untrue. In Fig. 4 the first value of $s(A)$ were from REACTLAB and the second value from SQUAD are in brackets.

(b) *Physical significance of species concentration* The distribution diagram of the relative concentrations of all species (Fig. 4) showed the protonation equilibrium of the differently protonated species L^-, LH, LH_2^+ and LH_3^{2+}. The graph showed that none of these species reached too low, and therefore chemically insignificant, concentrations; thus, all species have physicochemical significance in pH range from 2 to 9.

(c) *Sufficient goodness-of-fit of calculated spectra after regression* Statistical analysis of all residuals [49, 50] exhibited that the global minimum of the elliptic hyperparaboloid of the objective residual sum of squares *RSS* was reached (Table 1), because the values of the arithmetic mean of residuals $E(\hat{e})$ [mAU], standard deviations of residuals with $s(e)$ [mAU] and the average of absolute value of residuals $E(|\hat{e}|)$ reached very low values, all < 2 mAU, which actually represented < 0.2% of the measured value of the regressed dependent absorbance variable.

4.1.4 The Search for an Effective Range of Wavelengths (Fig. S1 in Supplementary Material)

For regression analysis, it was customary to use only the sufficiently efficient part of the spectra, which would make it easier to make estimates of unknown parameters. Three wavelength ranges of the analysed spectrum were selected, namely (a) 270–340 nm, (b) 270–310 nm and (c) 300–340 nm, in which the spectra were evaluated. Figure S1 illustrated estimates of three dissociation constants, including the goodness-of-fit test of the calculated spectra, expressed here as the standard deviation of absorbance $s(A)$. This statistic served as an objective criterion for the reliability of the calculated parameter estimates. The best fitness of the calculated spectra through experimental absorbance points of $s(A) = 2.22$ mAU (REACTLAB) and 1.15 mAU (SQUAD) was obtained in the wavelength range of 300–340 nm, although the estimates of dissociation constants were similar in all three tested wavelength ranges. Similarly, the three distribution diagrams of the relative concentration of differently protonated species in Fig. S1 are very similar.

4.1.5 Change in Absorbance Spectra During pH Titration Adjustment (Fig. S2 in Supplementary Material)

Figure S2 showed that pH adjustment did not cause significant changes in the bedaquiline spectra at all wavelengths of the spectrum in the same way, as some chromophores were not sufficiently affected by pH adjustment. The largest changes in the absorbance-pH curve were around the pH dissociation constants and there were no changes in absorbance in the pH range from 9 to 12. Figure S2-*upper graph* shows a spectrum of molar absorption coefficients as a function of wavelength for selected wavelengths for which A-pH curves have been shown. Figure S2-*lower graph* shows the sensitivity of the chromophores in the bedaquiline molecule to pH, which was monitored in the form of A-pH curves. The maximum change in absorbance on Fig. S2-*upper graph* occurred with pH changes at 274, 282,

290 nm as well as at 320 and 335 nm. The graphs yielded estimates of dissociation constants and the presence of predominantly differently protonated species. It was also obvious from these graphs that two dissociation constants $pK_{a1} = 3.68$ and $pK_a = 4.74$ were close, and therefore their estimation would be uncertain.

4.1.6 Signal-to-Noise Ratio in Spectral Change (Fig. S3 in Supplementary Material)

When making spectrophotometric determination of the dissociation constants of bedaquiline, it was necessary to investigate the hidden information in the spectral data to determine whether the titration change in pH caused a sufficient change in the spectral absorbance values for regression, to determine the dissociation constants and to build a protonation model. It was clear from Fig. S3 that the spectral response of the chromophore bedaquiline was not the same everywhere and was sufficient for the studied protonation equilibria. It was therefore necessary to verify whether the proposed three dissociation constants could be reliably estimated even with small changes in absorbance. This verification was based on a comparison of the spectral changes in absorbance during pH titration against residual sizes. When we expressed the absorbance difference in the *i*-th spectrum at the *j*-th value of its absorbance by the relation $\Delta_{ij} = A_{ij} - A_i$, it was necessary to investigate whether these small absorbance changes Δ_{ij} in the spectra were sufficiently large and mainly larger than the value of the absorbance noise, expressed here by the instrumental standard deviation of the absorbance, $s_{inst}(A) \sim 1$ mAU.

The oscillation of the absorbance difference Δ_{ij} in mAU in the spectra plotted versus the wavelength λ for all elements of the absorption matrix in Fig. S3-*upper graph* showed that the values of the absorbance change Δ_{ij} are smaller at some wavelengths, but still larger than the measured instrument noise, $s_{inst}(A) \sim 1$ mAU. Figure S3-*lower graph* confirmed the excellent fitness of the calculated regression spectra through the experimental points, since the residual sizes *e* are predominantly in the range of -5 to $+5$ mAU, while the absorbance changes Δ_{ij} in Fig. S3-*upper graph* are of higher magnitudes up to 750 mAU. The size of the residuals showed the degree of suitability of the A-pH curve for data analysis. Residuals should oscillate around zero and their $\pm$ sign should change with their frequent oscillations. Residuals should also exhibit a Gaussian distribution with the mean close to zero. For the best regression model, the standard deviation $s(A)$ is expected to be similar and close to the instrumental noise of absorbance, $s_{inst}(A)$.

4.1.7 The Spectra Deconvolution (Fig. S4 in Supplementary Material)

Deconvolution of each experimental spectrum into absorption bands of the individual differently protonated species showed whether the protonation hypothesis was designed efficiently. Figure S4 illustrates the deconvolution of selected experimental spectra into absorption bands of variously protonated bedaquiline species at pH (2.85, 2.99, 3.55, 4.45, 5.26, 5.43, 6.03 and 6.61).

At pH 2.85 and 2.99, the absorption bands of LH_3^{2+} cation is in equilibrium with LH_2^+ and showed that the chromophore significantly indicated a protonation equilibrium at wavelengths of 270–290 nm and also at 320–330 nm, where the absorbance's maximum λ_{max} can be indicated with its value ε_{max}. The indication of protonated cations continued over pH 3.55 up to pH 4.45, mainly at maxima of wavelengths of 320–330 nm. While from pH 2 to pH 4 the spectrum was dominated by the LH_3^{2+} cation in equilibrium with LH_2^+

cation, the neutral molecule LH with its weak absorption band did not absorb in this range because it was present in a very low concentration. From pH 4.45 the molecule LH started to show absorbance mainly at maxima of 320–330 nm and the weaker band appeared at a maximum of 290 nm. From pH 5.26, the absorption band of LH_2^+ cation decreased and at pH 6 it completely disappeared and the absorption band of the neutral molecule LH increased. From pH 6 to pH 7, the absorbance of the anion L^- appeared, which however, was not characterized by an absorption band with a maximum at the selected wavelength. The deconvolution of the spectra was of a significant aid in the discussion of the protonation scheme of the bedaquiline molecule.

4.2 pH-Metric Data Analysis

Potentiometric titration of acidified bedaquiline with potassium hydroxide was performed at 25 °C and 37 °C (Table 2) and at adjusted ionic strength (Fig. 5). When analyzing the pH-metric data, the initial estimate of each bedaquiline dissociation constant was adjusted by the ESAB program.

4.2.1 pH-Metric Data Analysed by Bjerrum's Formation Function

Bedaquiline has three dissociation constants and their refinement was performed by the nonlinear regression of the pH-metric titration curve using the ESAB program [12]. Nonlinear regression analysis was applied to the central part of the pH-metric titration curve for protonated cation of bedaquiline titrated with potassium hydroxide (Fig. 5). Estimates of the three dissociation constants pK_{a1}, pK_{a2} and pK_{a3} were evaluated on the base of the Bjerrum formation function curve. At a concentration higher than 2×10^{-4} mol·dm^{-3}, bedaquiline precipitate appeared in the solution. Residuals in ESAB program were defined as the difference between the experimental and calculated volume of titrant KOH, $e_i = V_{\mathrm{exp},I} - V_{\mathrm{calc},i}$. The reliability test of refined estimates of dissociation constants was performed by statistical analysis of residuals. Moreover, by regression improving the estimates of two *group parameters* H_0, L_0, the statistics of the goodness-of-fit improved significantly. The relatively sensitive reliability criterion of the estimated dissociation constants was the mean of the absolute value of residuals $E\left|\bar{e}\right|$ in μL. Comparing the numerical value of this statistic with the instrumental noise represented by the instrumental standard deviation of titrant KOH, $s_{\mathrm{inst}}(V) = s(V) = 0.1$ μL, excellent curve fitting was proven because the mean of absolute values of residuals $E\left|\hat{e}\right|$ and the residual standard deviation of the titrant KOH of $s(V)$ was equal to or lower than the experimental noise, $s_{\mathrm{inst}}(V)$. The values of both these monitored statistics 0.1 μL were similar to the instrumental error of the used microburettes $s(V) = 0.1$ μL. In addition, residuals oscillated between the lower (− 0.3 μL) and upper (+0.3 μL) limits of Hoaglin's internal boundaries, and no residual value was found outside these limits, see page 81 in the textbook [49]. Estimates of the dissociation constants refined by ESAB therefore proved to be sufficiently reliable (Table 2). The fitting of the curve could only be improved by further refining the parameter of the L_0 group, the concentration of bedaquiline drug in the titration vessel.

Table 2 Reproducibility of the best protonation model of bedaquiline in the pH range of 2–13 for the three dissociation constants pK_{a1}, pK_{a2}, pK_{a3} with ESAB was examined

Temperature	25 °C					37 °C				
Reproducibility	1st set	2nd set	3rd set	4rd set	Mean	1st set	2nd set	3rd set	4rd set	Mean
Estimates of the group parameters H_0, H_T and L_0 in the searched protonation model										
$H_0 \times$ 1E+02 [mol·dm^{-3}]	6.53	7.65	7.87	7.17		6.57	7.65	7.20	7.25	
$L_0 \times$ 2E+04 [mol·dm^{-3}]	0.97	1.23	1.98	2.54		1.45	0.92	0.25	1.88	
Estimates of the common parameters i.e. dissociation constants in the searched protonation model										
pK_{a1}, $LH_3^{2+} \rightleftharpoons H^+ + LH_2^+$	3.16	3.19	3.15	3.34	3.21	3.28	3.27	3.274	3.38	3.30
pK_{a2}, $LH_2^+ \rightleftharpoons H^+ + LH$	3.89	3.49	3.78	3.55	3.68	3.69	3.65	4.11	3.76	3.80
pK_{a3}, $LH \rightleftharpoons H^+ + L^-$	5.24	5.22	5.23	5.16	5.21	4.34	4.35	4.45	4.55	4.42
Goodness-of-fit test with the statistical analysis of residuals										
Mean of absolute value of residuals, $E\left\vert \hat{e} \right\vert$ [µL]	0.281	0.145	0.145	0.401		0.242	0.341	0.387	0.416	
Residual standard deviation, $s(\hat{e})$, [µL]	0.383	0.178	0.183	0.564		0.316	0.454	0.432	0.531	
Akaike-Information Criterion, *AIC*	− 293.0	− 339.4	− 305.8	− 323.1		− 332.5	− 332.7	− 257.4	− 295.6	
Hamilton R-factor from ESAB [%]	0.0332	0.0132	0.0145	0.0443		0.0276	0.0335	0.0340	0.0416	

The regression refinement of common and group parameters for pH-metric titration of acidified 2.0×10^{-4} mol· dm^{-3} bedaquiline, which was titrated with potassium hydroxide at 25.0 °C and 37.0 °C. The reliability of parameter estimation was proven with goodness-of-fit statistics: the mean of absolute value of residuals, $E\left\vert \hat{e} \right\vert$ in µL, the standard deviation of residuals $s(\hat{e})$ in µL, the Hamilton *R-factor* of relative fitness [%] from ESAB and the Akaike-Information Criterion *AIC*. Common parameters refined: pK_{a1}, pK_{a2}, pK_{a3}. Group parameters refined: H_0, L_0. Constants: $t = 25.0$ °C, 37.0 °C, $pK_w = 13.9799$, $s(V) = s_{inst}(y) = 0.1$ µL, I_0 adjusted (in vessel), $H_T = I_T = 0.9470$ (in burette KOH)

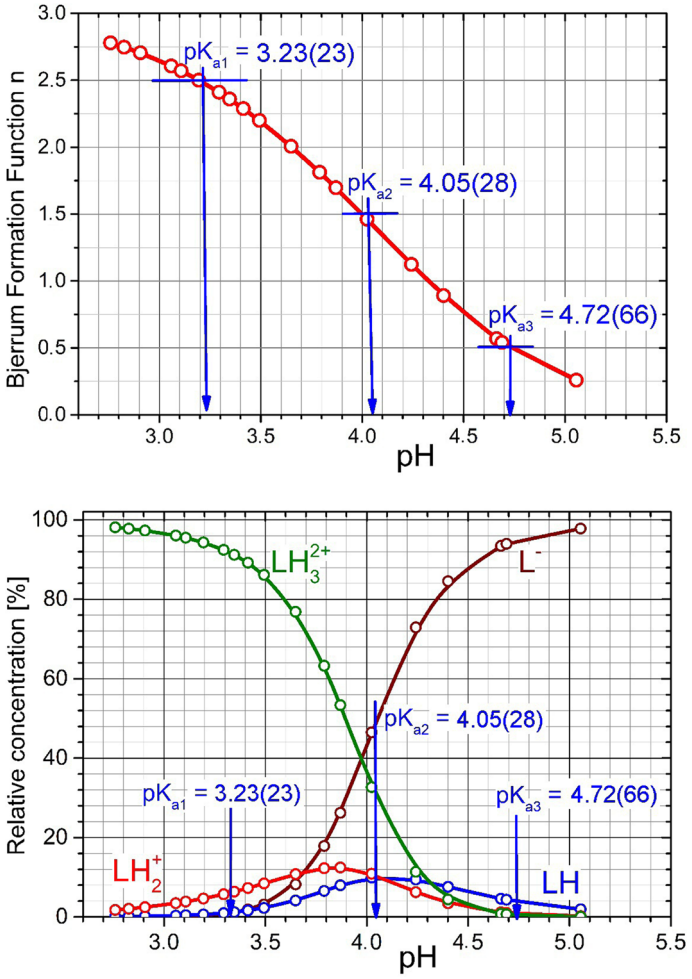

Fig. 5 *Upper graph* The pH-metric data of bedaquiline, analyzed by Bjerrum's formation function in the pH-titration of acidified bedaquiline to pH 2, which was titrated with potassium hydroxide at 25 °C and resulted in three dissociation constants in the pH range 3–5.5. The standard deviation of the pK_a estimate in the last valid place of the estimate are given in parentheses. *Lower graph* The distribution diagram of the relative concentrations of the differently protonated bedaquiline species in % also contains the estimates of three dissociation constants

4.2.2 Uncertainty of pK_{ai} in Reproduced Measurements (Figs. S5 and S6 in Supplementary Material)

The reproducibility of the dissociation constants evaluated by REACTLAB from the four replicate measurements was found to be in good agreement as shown in Table 1. The interpretation would be as follows:

(a) The estimate of the mean of the four reproduced dissociation constants served as a measure of the uncertainty for each dissociation constant.
(b) At 37 °C, the estimates of the dissociation constant were slightly more acidic, i.e. they exhibited lower pK_a values than estimates at 25 °C.
(c) Very close values of two consecutive dissociation constants pK_{a1} and pK_{a2} could lead to some difficulties in the minimizing process. Reasons for this may be that the intermediate species was not present in a sufficiently high concentration, or that too close dissociation constants pK_{a1} and pK_{a2}, of one species were highly correlated with the pK_a of another one and so these two species would have the same effect on pH change.
(d) When the normal equations were singular, one or more correlation coefficients between the two parameters pK_{a1} and pK_{a2} were nearly close to one or minus one, so that the refinement process could be terminated too early [49].

4.2.3 Thermodynamic Dissociation Constants

Using the Debye–Hückel equation for the data, the unknown parameters pK^T_{a1}, pK^T_{a2}, and pK^T_{a3} were estimated at two temperatures of 25 °C and 37 °C. Due to the narrow range and low values of the ionic strength, which was adjusted with KCl, two parameters could not be calculated, namely the ion size parameter *å* and the salinity coefficient *C*: $pK^T_{a1}=3.91(09)$, $pK^T_{a2}=4.58(12)$ and $pK^T_{a3}=5.26(07)$ at 25 °C and $pK^T_{a1}=3.61(30)$, $pK^T_{a2}=4.44(15)$ and $pK^T_{a3}=5.54(33)$ at 37 °C (spectrophotometry) and $pK^T_{a1}=3.21(39)$, $pK^T_{a2}=3.68(31)$ and $pK^T_{a3}=5.21(42)$ at 25 °C and $pK^T_{a1}=3.31(12)$, $pK^T_{a2}=3.67(15)$ and $pK^T_{a3}=5.73(08)$ at 37 °C (potentiometry).

4.2.4 Determination of Enthalpy, Entropy and Gibbs Energy for Dissociation (Figs. S7 and S8 in Supplementary Material)

The change in the standard state enthalpy ΔH^0 of the dissociation process was calculated from the van't Hoff equation $d\ln K/dT=\Delta H^0/RT^2$. From the values of Gibbs energy $\Delta G^0=-RT\ln K$ and enthalpy ΔH^0 we can calculate the entropy $\Delta S^0=(\Delta H^0-\Delta G^0)/T$, where R (ideal gas constant) $=8.31451\ J\cdot K^{-1}\cdot mol^{-1}$, where K is the thermodynamic dissociation constant and T is the absolute temperature.

For bedaquiline, with increasing temperatures ranging from 15 to 50 °C, the values of all dissociation constants, determined spectrophotometrically (Fig. S7-*upper graph*) and potentiometric-cally (Fig. S7-*lower graph*), decrease. The temperature response of all three dissociation constants pK_{a1}, pK_{a2} and pK_{a3} was more pronounced in the pH-metric analysis, the correlation coefficients of the dissociation constant versus temperature were significantly higher than in the UV-metric spectral analysis (Fig. S8).

4.2.4.1 UV-Metric Spectral Analysis Estimations of dissociation constants from pH-absorbance spectral data were used to calculate extra-thermodynamics (Fig. 6). Positive values of enthalpy $\Delta H^0(pK_{a1})=9.11\ kJ\cdot mol^{-1}$, $\Delta H^0(pK_{a2})=13.76\ kJ\cdot mol^{-1}$, and $\Delta H^0(pK_{a3})=67.17\ kJ\cdot mol^{-1}$ at 25 °C showed that the dissociation process is endothermic and is accompanied by heat absorption.

4.2.4.2 pH-Metric Analysis Estimations of dissociation constants from pH-titration data were used to calculate extra-thermodynamics (Fig. 7). Positive values of enthalpy $\Delta H^0(pK_{a1})=85.49\ kJ\cdot mol^{-1}$, $\Delta H^0(pK_{a2})=86.42\ kJ\cdot mol^{-1}$, and $\Delta H^0(pK_{a3})=65.84\ kJ\cdot mol^{-1}$

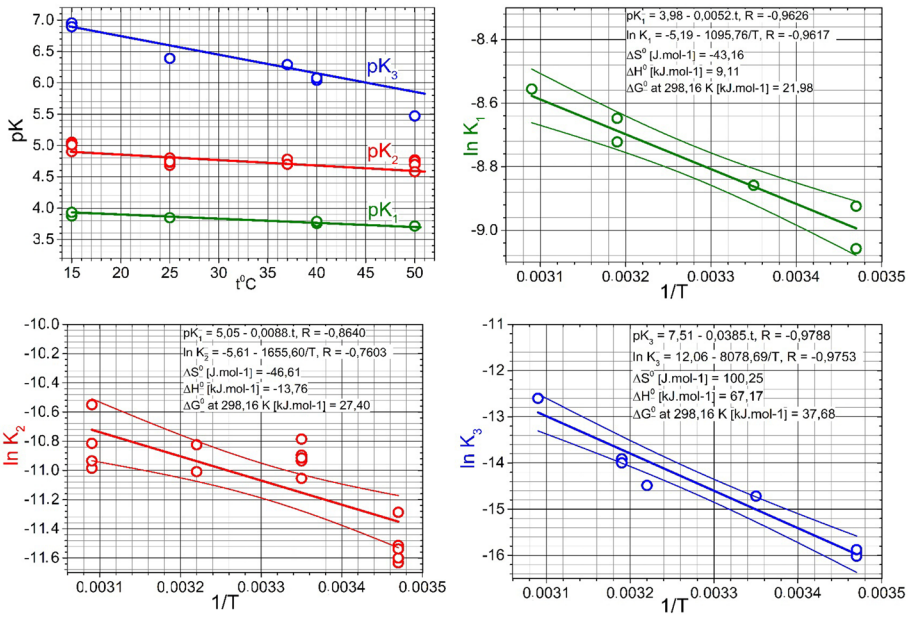

Fig. 6 The working diagram of the three dissociation constants on the temperature ln $K = f(1/T)$ showing the linear dependence evaluated by linear regression analysis of spectrophotometric data

at 25 °C showed that the dissociation process is endothermic and is accompanied by heat absorption.

5 Discussion

The REACTLAB regression program analyzed an absorbance matrix of pH for 1×10^{-4} mol·dm^{-3} bedaquiline and estimated two dissociation constants using two different numerical approaches. The results of refinement of the dissociation constant may include information regarding a good fit of the residual sum function of the squares *RSS*, the estimated parameters, the standard deviations of the parameters and the correlation coefficients between them, the residual maps and concentration of all species in the model for all data points. Model selection [50] was the process of deciding whether to accept the regression results. Usually, all of the above factors need to be considered, as none of them is a reliable indicator of the success or failure of the calculation in itself. The ESAB program minimized the residuals $e_i = V_{\text{exp},\,i} - V_{\text{calc},i}$, reached residual values of about 0.1 or 0.2 µL, which means that an excellent curve of the calculated titration curve is calculated to have been fitted through the experimental points. It can be stated that the reliability of bedaquiline dissociation constants was proven, even though the group parameters L_0, H_T were poorly conditioned in the nonlinear regression model.

The inconsistency of the experimentally obtained estimates of pK_{ai} with their theoretically predicted values could be due to the complex resonance structure of the heterocyclic nucleus and consequently to different electron distributions, which could further lead to

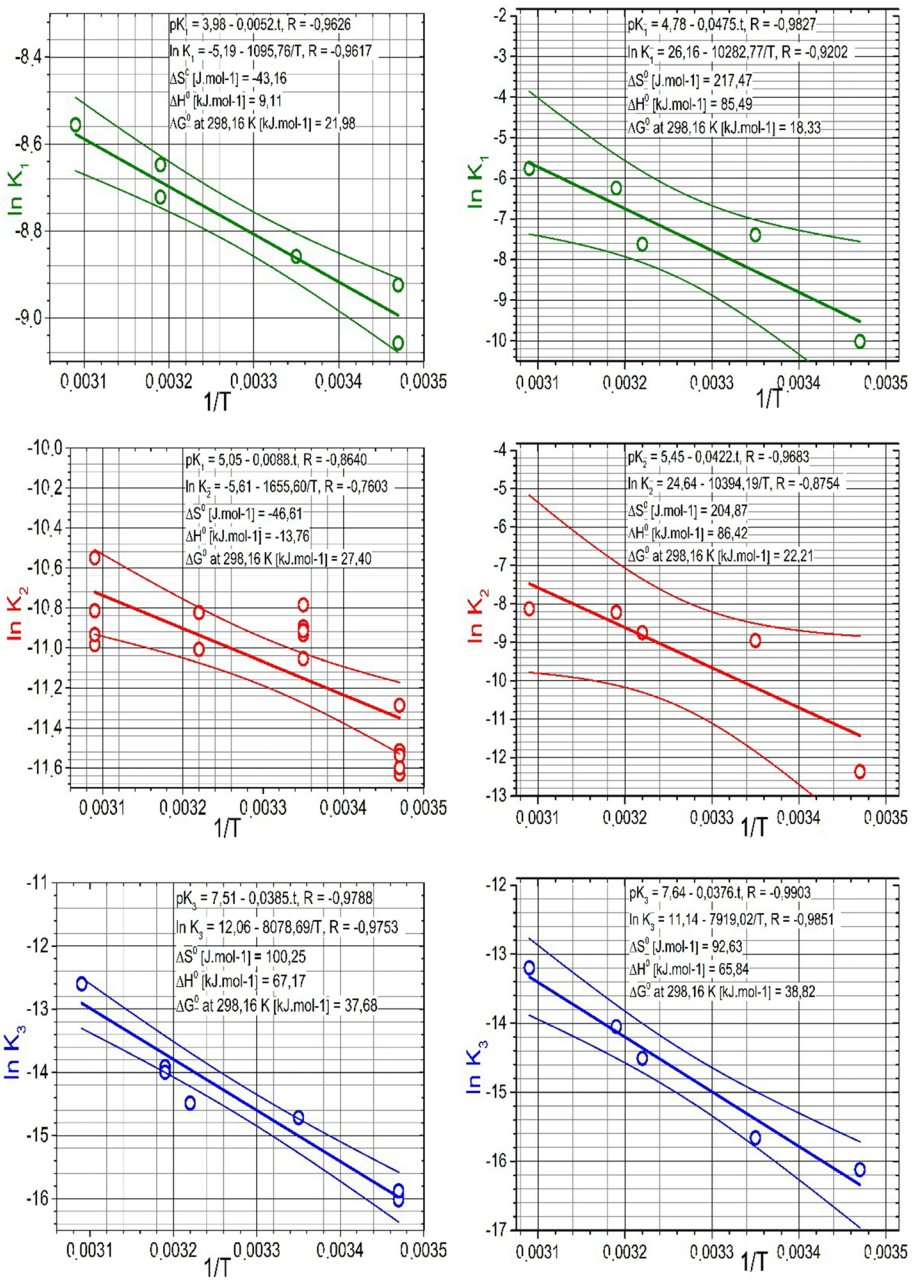

Fig. 7 The linear dependence of the estimates of three mixed dissociation constants on the temperature $pK_a = f(t\ ^\circ C)$ was transformed into the new coordinates $\ln K = f(1/T)$. The standard state molar enthalpy ΔH^0, the molar entropy ΔS^0 and the molar Gibbs energy ΔG^0 were calculated from the intercept and slope of the regression straight line of the temperature dependence, measured (*left graphs*) with UV-metric spectral analysis and (*right graphs*) with pH-metric analysis. The straight lines were drawn with the Working-Hotteling confidence bands (QCEXPERT)

different predicted pK_{ai} values according to the structural formula of the molecule. In such cases, the prognostic programs MARVIN, PALLAS and ACD/Percepta could fail and the dissociation constants would certainly have to be determined experimentally.

(1) If pK_a is positive, the standard change of Gibbs energy ΔG^0 for the dissociation reaction is also positive. A positive ΔH^0 value indicates that the dissociation process is endothermic and is accompanied by heat absorption. The hydrogen bond rearrangement could then be the basis for both ΔH^0 and ΔS^0 in drug–proton interactions, and the relationship between ΔH^0 and ΔS^0 appears plausible, indeed likely. Hydrogen bonding as a central drug–proton interaction is also mechanistically attractive. In water, hydrogen bonds form a network of continuous chains that change dynamically (in a certain state). Because of the dipole formed by the displacement of an electron from a hydrogen proton, these chains form a sequence of mono- and di-poles that are sensitive to the electrostatic potential of the drug and receptor molecules and provide a mechanism for the transmission of information at a distance from the drug to the receptor.
(2) The contribution of entropy is mostly unfavorable in these reactions ($\Delta S^0 < 0$). The ions in the aqueous solution tend to orient the surrounding water molecules, which order the solution and reduce its entropy. The contribution of an ion to entropy is a partial molar entropy, which is often negative, especially for small or highly charged ions. Acid ionization involves the reversible formation of two ions, so the entropy decreases ($\Delta S^0 < 0$). There are now two anions for reversible ionization, so the entropy decreases again.

6 Conclusions

(1) Spectrophotometric and potentiometric pH titration allowed the measurement of up to two narrow dissociation constants of bedaquiline (Scheme 1). Bedaquiline chromophores showed minimal changes in absorbance in the UV/VIS spectra when adjusting the pH of the solution, and therefore estimates of dissociation constants were subject to greater uncertainty than potentiometric determinations. Therefore, a more reliable estimate of the dissociation constants obtained potentiometrically has emerged.
(2) The bedaquiline neutral molecule labelled LH was capable of protonation and dissociation in pure water to form soluble species L^-, LH, LH_2^+, LH_3^{2+} and LH_4^{3+}. The graph of molar absorption coefficients of differently protonated species in relation to the wavelength indicated that the spectra of ε_L, ε_{LH}, ε_{LH2}, ε_{LH3} and ε_{LH4} were correlated for the species and that the values in pairs were almost the same.
(3) It has been shown that in the pH range 2–7, two dissociation constants can be reliably estimated from the spectrum when the concentration of sparingly soluble bedaquiline was 1.0×10^{-4} mol·dm^{-3} or less. Although the adjusted pH had less effect on the changes in absorbance in the chromophore, two thermodynamic dissociation constants were reliably determined, with REACTLAB reaching $pK_{a1}^T = 3.91$ (09), $pK_{a2}^T = 4.58$ (12) and $pK_{a3}^T = 5.26$ (07) at 25 °C and $pK_{a1}^T = 3.61$ (30), $pK_{a2}^T = 4.44$ (15) and $pK_{a3}^T = 5.54$ (33) at 37 °C.
(4) The three thermodynamic dissociation constants of bedaquiline were determined by regression analysis of the potentiometric pH-titration curves at a concentration of

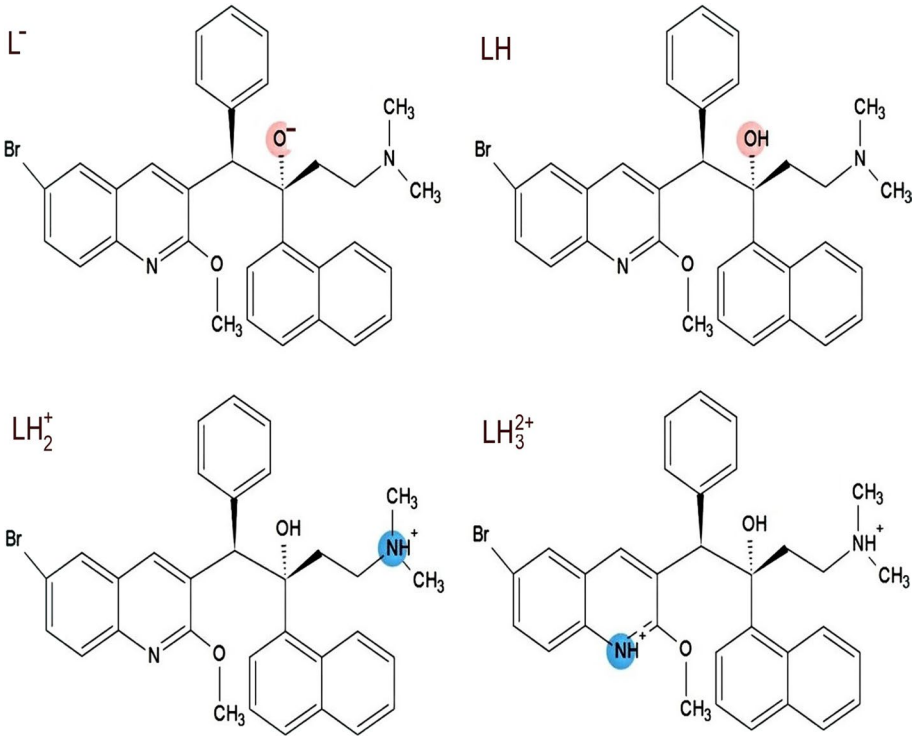

Scheme 1 Protonation scheme of bedaquiline

1×10^{-3} mol·dm^{-3} with ESAB, $pK_{a1}^{T} = 3.21$ (39), $pK_{a2}^{T} = 3.68$ (31) and $pK_{a3}^{T} = 5.21$ (42) at 25 °C and $pK_{a1}^{T} = 3.31$ (12), $pK_{a2}^{T} = 3.67$ (15) and $pK_{a3}^{T} = 5.73$ (08) at 37 °C.

(5) "Extra-thermodynamics" of dissociation from the UV-metric analysis: To calculate the extra-thermodynamics of the spectral data, the positive values of enthalpy were $\Delta H^0(pK_{a1}) = 9.11$ kJ·mol^{-1}, $\Delta H^0(pK_{a2}) = 13.76$ kJ·mol^{-1}, $\Delta H^0(pK_{a3}) = 67.17$ kJ·mol^{-1} and showed that the dissociation process is endothermic and is accompanied by heat absorption.

"Extra-thermodynamics" of dissociation from the pH-metric analysis: To calculate the extra-thermodynamics of the potentiometric data, the positive values of enthalpy were $\Delta H^0(pK_{a1}) = 85.49$ kJ·mol^{-1}, $\Delta H^0(pK_{a2}) = 86.42$ kJ·mol^{-1}, $\Delta H^0(pK_{a3}) = 65.84$ kJ·mol^{-1} and showed that the dissociation process is endothermic and is accompanied by heat absorption.

(6) Prediction of bedaquiline dissociation constants was performed by MARVIN, PALLAS and ACD/Percepta programs for determination of protonation sites. When comparing the three predictive and two experimental techniques, the prognostic programs sometimes differed in their pK_a estimations.

Supplementary Information The online version contains supplementary material available at https://doi.org/10.1007/s10953-021-01055-w.

References

1. Wikipedia: Bedaquiline. Wikipedia-https://pubchem.ncbi.nlm.nih.gov/compound/Bedaquiline (2013)
2. Multum, C.: Bedaquiline. Drugs.com https://www.drugs.com/mtm/Bedaquiline.html (2020)
3. Prakash, S.: Pharmacovigilance in India. Indian J. Pharmacol. **39**(3), 1 (2007). https://doi.org/10.4103/0253-7613.33430
4. Sarathy, J.P., Gruber, G., Dick, T.: Re-Understanding the mechanisms of action of the anti-mycobacterial drug bedaquiline. Antibiotics **8**(4), 261–273 (2019). https://doi.org/10.3390/antibiotics8040261
5. Koul, A., Dendouga, N., Vergauwen, K., Molenberghs, B., Vranckx, L., Willebrords, R., Ristic, Z., Lill, H., Dorange, I., Guillemont, J., Bald, D., Andries, K.: Diarylquinolines target subunit C of mycobacterial ATP synthase. Nat. Chem. Biol. **3**(6), 323–324 (2007). https://doi.org/10.1038/nchembio884
6. Segala, E., Sougakoff, W., Nevejans-Chauffour, A., Jarlier, V., Petrella, S.: New mutations in the mycobacterial ATP synthase: new insights into the minding of the diarylquinoline TMC207 to the ATP synthase C-ring structure. Antimicrob. Agents Chemother. **56**(5), 2326–2334 (2012). https://doi.org/10.1128/AAC.06154-11
7. Goldberg, R.N., Kishore, N., Lennen, R.M.: Thermodynamic quantities for the ionization reactions of buffers. J. Phys. Chem. Ref. Data **31**(2), 231–370 (2002). https://doi.org/10.1063/1.1416902
8. Williams, H.D., Trevaskis, N.L., Charman, S.A., Shankere, R.M., Charman, W.N., Pouton, C.E., Porter, C.J.H.: Strategies to address low drug solubility in discovery and development. Pharmacol. Rev. **65**(1), 315–499 (2013). https://doi.org/10.1124/pr.112.005660
9. Al-Bedair, L.A.: Potentiometric studies on the binary and mixed ligand complexes in solution: Zn(II)–amlodipine–amino acids systems. Orient. J. Chem. **32**(1), 609–615 (2016). https://doi.org/10.13005/Ojc/320169
10. Alderighi, L., Gans, P., Lenco, A., Peters, D., Sabatini, A., Vacca, A.: Hyperquad simulation and speciation (HySS): a utility program for the investigation of equilibria involving soluble and partially soluble species. Coord. Chem. Rev. **184**, 311–318 (1999). https://doi.org/10.1016/S0010-8545(98)00260-4
11. Byrne, L.A., Hynes, M.J., Connolly, C.D., Murphy, R.A.: Analytical determination of apparent stability constants using a copper ion selective electrode. J. Inorg. Biochem. **105**(12), 1656–1661 (2011). https://doi.org/10.1016/j.jinorgbio.2011.07.016
12. De Stefano, C., Princi, P., Rigano, C., Sammartano, S.: Computer analysis of equilibrium data in solution ESAB2M: an improved version of the ESAB program. Ann. Chim. **77**(7–8), 643–675 (1987)
13. Gans, P., Sabatini, A., Vacca, A.: Investigation of equilibria in solution. Determination of equilibrium constants with the HYPERQUAD suite of programs. Talanta **43**(10), 1739–1753 (1996). https://doi.org/10.1016/0039-9140(96)01958-3
14. Gans, P., Sabatini, A., Vacca, A.: Hyperquad computer-program suite. Abstr. Pap. Am. Chem. Soc. **219**, U763–U763 (2000)
15. Gans, P., Sabatini, A., Vacca, A.: Simultaneous calculation of equilibrium constants and standard formation enthalpies from calorimetric data for systems with multiple equilibria in solution. J. Solution Chem. **37**(4), 467–476 (2008). https://doi.org/10.1007/s10953-008-9246-6
16. Allen, R.I., Box, K.J., Comer, J.E.A., Peake, C., Tam, K.Y.: Multiwavelength spectrophotometric determination of acid dissociation constants of ionizable drugs. J. Pharm. Biomed. Anal. **17**(4–5), 699–712 (1998). https://doi.org/10.1016/S0731-7085(98)00010-7
17. Meloun, M., Ferenčíková, Z., Niesnerová, I., Pekárek, T.: Oligomers-model building in protonation equilibria of sitagliptin. Cent. Eur. J. Chem. **11**(11), 1799–1807 (2013). https://doi.org/10.2478/s11532-013-0304-6
18. Krotz-Vogel, W., Hoppe, H.C.: The PALLAS parallel programming environment. Lect. Notes Comput. Sci. **1332**, 257–266 (1997). https://doi.org/10.1007/3-540-63697-8_93
19. Krotz-Vogel, W., Hoppe, H.C.: PALLAS parallel tools—a uniform programming environment from workstations to teraflop computers. Adv. Parallel Comput. **12**, 349–358 (1998)
20. Meloun, M., Syrový, T., Bordovská, S., Vrána, A.: Reliability and uncertainty in the estimation of pK(a) by least squares nonlinear regression analysis of multiwavelength spectrophotometric pH titration data. Anal. Bioanal. Chem. **387**(3), 941–955 (2007). https://doi.org/10.1007/s00216-006-0993-1
21. Japertas, P., Lanevskij, K., Sazonovas, A.: ACD/Percepta structure design engine: virtual enumeration and screening of physchem properties for 10(16) compounds in real time. Abstr. Pap. Am. Chem. Soc. **248** (2014)
22. ACD/p*K*a DB. In: p*K* Prediction Software. Advanced Chemistry Development, Inc., Toronto, Canada (2021). https://www.acdlabs.com
23. ACD/Labs p*K*a Predictor 3.0. In: Inc., A.C.D. (ed.) Toronto, Canada (2007). https://www.acdlabs.com, 2021

24. Balogh, G.T., Gyarmati, B., Nagy, B., Molnar, L., Keseru, G.M.: Comparative evaluation of in silico p*K*(a) prediction tools on the gold standard dataset. Qsar Comb. Sci. **28**(10), 1148–1155 (2009). https://doi.org/10.1002/gsar.200960036
25. ChemAxon: MARVINSketch 4.1.8. In: ChemAxon, 2007. MarvinSketch 4.1.8. XhemAxon Kft. Budapest, Hungary. http://www.chemaxon.com/products.html, vol. 2007. ChemAxon, 2007 XhemAxon Kft. Budapest, Hungary (2007)
26. Meloun, M., Bordovská, S., Syrový, T.: A novel computational strategy for the p*K*(a) estimation of drugs by non-linear regression of multiwavelength spectrophotometric pH-titration data exhibiting small spectral changes. J. Phys. Org. Chem. **20**(9), 690–701 (2007). https://doi.org/10.1002/poc.1235
27. Manchester, J., Walkup, G., Rivin, O., You, Z.P.: Evaluation of p*K*(a) estimation methods on 211 drug like compounds. J. Chem. Inf. Model. **50**(4), 565–571 (2010). https://doi.org/10.1021/ci100019p
28. Meloun, M., Bordovská, S.: Benchmarking and validating algorithms that estimate p*K*(a) values of drugs based on their molecular structures. Anal. Bioanal. Chem. **389**(4), 1267–1281 (2007). https://doi.org/10.1007/s00216-007-1502-x
29. Meloun, M., Bordovská, S., Syrový, T., Vrána, A.: Tutorial on a chemical model building by least-squares non-linear regression of multiwavelength spectrophotometric pH-titration data. Anal. Chim. Acta **580**(1), 107–121 (2006). https://doi.org/10.1016/j.aca.2006.07.043
30. Meloun, M., Čápová, A., Pilařová, L., Pekárek, T.: Multiwavelength UV-metric and pH-metric determination of the multiple dissociation constants of the Lesinurad. J. Pharm. Biomed. Anal. **158**, 236–246 (2018). https://doi.org/10.1016/j.jpba.2018.05.047
31. Meloun, M., Havel, J., Högfeldt, E.: Computation of Solution Equilibria: A Guide to Methods in Potentiometry, Extraction, and Spectrophotometry. Ellis Horwood Series in Analytical Chemistry. Ellis Horwood, Chichester (1988)
32. Rodante, F., Fantauzzi, F.: Thermodynamic analysis of the ionization of ortho and para toluic acids—influence of the medium on the hyperconjugative and steric effects. Thermochim. Acta **109**(2), 353–365 (1987). https://doi.org/10.1016/040-6031(87)80031-X
33. Meloun, M., Ferenčíková, Z.: Enthalpy–entropy compensation for some drugs dissociation in aqueous solutions. Fluid Phase Equil. **328**, 31–41 (2012). https://doi.org/10.1016/j.fluid.2012.05.011
34. Debnath, A.K., Shusterman, A.J., Decompadre, R.L.L., Hansch, C.: The importance of the hydrophobic interaction in the mutagenicity of organic-compounds. Mutat. Res. **305**(1), 63–72 (1994). https://doi.org/10.1016/0027-5107(94)90126-0
35. Gruber, C., Buss, V.: Quantum mechanically calculated properties for the development of quantitative structure–activity–relationships (Qsars)—p*K*a values of phenols and aromatic and aliphatic carboxylic-acids. Chemosphere **19**(10–11), 1595–1609 (1989). https://doi.org/10.1016/0045-6535(89)90503-1
36. Shusterman, A.J.: Predicting mutagenicity—use a technique thats been useful in predicting efficacy. ChemTech **21**(10), 624–627 (1991)
37. Trapani, G., Carotti, A., Franco, M., Latrofa, A., Genchi, G., Liso, G.: Structure affinity relationships of some alkoxycarbonyl-2h-pyrimido[2,1-B]benzothiazol-2-ones or alkoxycarbonyl-4h-pyrimido[2,1-B]benzothiazol-4-ones benzodiazepine receptor ligands. Eur. J. Med. Chem. **28**(1), 13–21 (1993). https://doi.org/10.1016/0223-5234(93)90074-O
38. Aguerre, R.J., Suarez, C., Viollaz, P.E.: Enthalpy–entropy compensation in sorption phenomena—application to the prediction of the effect of temperature on food isotherms. J. Food Sci. **51**(6), 1547–1549 (1986). https://doi.org/10.1111/j.1365-2621.1986.tb13856.x
39. Gabas, A.L., Telis-Romero, J., Menegalli, F.C.: Thermodynamic models for water sorption by grape skin and pulp. Dry. Technol. **17**(4–5), 961–974 (1999). https://doi.org/10.1080/07373939908917584
40. Labuza, T.P.: Enthalpy–entropy compensation in food reactions. Food Technol-Chicago **34**(2), 67–77 (1980)
41. Liu, L., Guo, Q.X.: Isokinetic relationship, isoequilibrium relationship, and enthalpy–entropy compensation. Chem. Rev. **101**(3), 673–695 (2001). https://doi.org/10.1021/cr990416z
42. Meloun, M., Nečasová, V., Javůrek, M., Pekárek, T.: The dissociation constants of the cytostatic bosutinib by nonlinear least-squares regression of multiwavelength spectrophotometric and potentiometric pH-titration data. J. Pharm. Biomed. Anal. **120**, 158–167 (2016). https://doi.org/10.1016/j.jpba.2015.12.012
43. Meloun, M., Pilařová, L., Čápová, A., Pekárek, T.: The overlapping thermodynamic dissociation constants of the antidepressant vortioxetine using UV-vis multiwavelength pH-titration data. J. Solution Chem. **47**(5), 806–826 (2018). https://doi.org/10.1007/s10953-018-0757-5
44. Meloun, M., Říha, V., Žáček, J.: Piston microburette for dosing aggressive liquids. Chem. Listy **82**(7), 765–767 (1988)

45. Leggett, D.J., McBryde, W.A.E.: General computer program for the computation of stability constants from absorbance data. Anal. Chem. **47**(7), 1065–1070 (1975). https://doi.org/10.1021/ac60357a046
46. Maeder, M., King, P.: Analysis of chemical processes, determination of the reaction mechanism and fitting of equilibrium and/or rate constants. In: Varmuza, K. (ed.) Chemometrics in Practical Applications, pp.41–62. Rjeka, InTech
47. Meloun, M., Čapek, J., Mikšík, P., Brereton, R.G.: Critical comparison of methods predicting the number of components in spectroscopic data. Anal. Chim. Acta **423**(1), 51–68 (2000). https://doi.org/10.1016/S0003-2670(00)01100-4
48. ORIGIN. In. OriginLab Corporation, One Roundhouse Plaza, Suite 303, Northampton, MA 01060, USA
49. Meloun, M., Militký, J.: Statistical Data Analysis: A Practical Guide, Complete with 1250 exercises and answer key on CD, 1st edn. Woodhead Publishing Limited, 80 High street Sawstone Cambridge, CB22 3HJ, UK, New Delhi, Cambridge, Oxford, Philadelphia (2011)
50. Meloun, M., Militký, J., Forina, M.: Chemometrics for Analytical Chemistry. PC-Aided Regression and Related Methods, vol. 2. Ellis Horwood, Chichester (1994), ISBN 0-13-123788-7

Terms and Conditions

Springer Nature journal content, brought to you courtesy of Springer Nature Customer Service Center GmbH ("Springer Nature").

Springer Nature supports a reasonable amount of sharing of research papers by authors, subscribers and authorised users ("Users"), for small-scale personal, non-commercial use provided that all copyright, trade and service marks and other proprietary notices are maintained. By accessing, sharing, receiving or otherwise using the Springer Nature journal content you agree to these terms of use ("Terms"). For these purposes, Springer Nature considers academic use (by researchers and students) to be non-commercial.

These Terms are supplementary and will apply in addition to any applicable website terms and conditions, a relevant site licence or a personal subscription. These Terms will prevail over any conflict or ambiguity with regards to the relevant terms, a site licence or a personal subscription (to the extent of the conflict or ambiguity only). For Creative Commons-licensed articles, the terms of the Creative Commons license used will apply.

We collect and use personal data to provide access to the Springer Nature journal content. We may also use these personal data internally within ResearchGate and Springer Nature and as agreed share it, in an anonymised way, for purposes of tracking, analysis and reporting. We will not otherwise disclose your personal data outside the ResearchGate or the Springer Nature group of companies unless we have your permission as detailed in the Privacy Policy.

While Users may use the Springer Nature journal content for small scale, personal non-commercial use, it is important to note that Users may not:

1. use such content for the purpose of providing other users with access on a regular or large scale basis or as a means to circumvent access control;
2. use such content where to do so would be considered a criminal or statutory offence in any jurisdiction, or gives rise to civil liability, or is otherwise unlawful;
3. falsely or misleadingly imply or suggest endorsement, approval , sponsorship, or association unless explicitly agreed to by Springer Nature in writing;
4. use bots or other automated methods to access the content or redirect messages
5. override any security feature or exclusionary protocol; or
6. share the content in order to create substitute for Springer Nature products or services or a systematic database of Springer Nature journal content.

In line with the restriction against commercial use, Springer Nature does not permit the creation of a product or service that creates revenue, royalties, rent or income from our content or its inclusion as part of a paid for service or for other commercial gain. Springer Nature journal content cannot be used for inter-library loans and librarians may not upload Springer Nature journal content on a large scale into their, or any other, institutional repository.

These terms of use are reviewed regularly and may be amended at any time. Springer Nature is not obligated to publish any information or content on this website and may remove it or features or functionality at our sole discretion, at any time with or without notice. Springer Nature may revoke this licence to you at any time and remove access to any copies of the Springer Nature journal content which have been saved.

To the fullest extent permitted by law, Springer Nature makes no warranties, representations or guarantees to Users, either express or implied with respect to the Springer nature journal content and all parties disclaim and waive any implied warranties or warranties imposed by law, including merchantability or fitness for any particular purpose.

Please note that these rights do not automatically extend to content, data or other material published by Springer Nature that may be licensed from third parties.

If you would like to use or distribute our Springer Nature journal content to a wider audience or on a regular basis or in any other manner not expressly permitted by these Terms, please contact Springer Nature at

onlineservice@springernature.com